

How does node centrality in a complex network affect prediction?*

Yuhong Xu[†] Xinyao Zhao[‡]

May 8, 2023

Abstract: In complex financial networks, systemically important nodes usually play vital roles. We consider networks consisting of major global assets and explore how node centrality affects price forecasting by applying a hybrid random forest algorithm. We find two counterintuitive phenomena: (i) factors with low centrality have better forecasting ability and (ii) nodes with low centrality can be predicted more accurately in direction. Using the notion of entropy, which measures the quantity of information, we show that factors with low centrality have more useful information and less noise for the forecast asset price than those with high centrality do. In addition, while predicting a systemically unimportant node, we demonstrate that the other nodes within the network have a higher information rate. Finally, we verify the robustness of our results using an alternative deep learning method.

Keywords: Complex network; Node centrality; Price forecasting; Machine learning; Information theory

1 Introduction

Applications of complex networks in finance include correlation analysis of financial markets (Ha et al. (2022); Wang et al. (2018)), risk management (Battiston et al. (2016); Yu and Zhao (2020); Ma et al. (2022)), asset allocation (Pozzi et al. (2013); Peralta and Zareei (2016); V́yrost et al. (2019); Olmo (2021)), trading behavior analysis (Adamic et al. (2017); Musciotto, et al. (2021)), and so on. In a financial system, systemically important financial institutions usually have a vital impact on other institutions and the entire system. For instance, if systemically important institutions are exposed to risk, the risk will be easily transmitted to others. Hence, effectively and accurately identifying them contributes to the regulation and control of risks. In recent years, many scholars have adopted complex

*The authors are listed in alphabetical order; and all authors made equal contributions.

[†]Center for Financial Engineering and Math Center for Interdiscipline Research, School of Mathematical Sciences, Soochow University, P. R. China. This work is supported by the Natural Science Foundation of China (No.12271391; No.11871050) and the Tang Scholar Fund.

[‡]Corresponding author. Center for Financial Engineering, School of Mathematical Sciences, Soochow University, P. R. China. Email: xyzhao1996@stu.suda.edu.cn.

networks and their centrality measures to capture the institutions (Chen et al. (2022); Kuzubas et al. (2014)).

Most recently, three US banks (Silver Gate Bank, Silicon Valley Bank, and Signature Bank) collapsed and Credit Suisse was acquired. Unlike the three US banks, Credit Suisse is listed as one of the global systemically important banks by the Financial Stability Board. Asset price forecasting is important for describing the evolution of financial networks. Naturally, we wonder whether there is a relationship between topological structure, especially node centrality, and forecasting effectiveness. Suppose that we enclose a set of assets in a complex network and consider two problems. (i) Is the forecasting accuracy with high central nodes as factors better than that with low central nodes as factors? Intuitively, nodes with high centrality should have more information about the entire system so they can better forecast an asset price. (ii) Are *systemically important nodes* (nodes with high centrality) more predictable than *systemically unimportant nodes* (nodes with low centrality)? We find that this is not the case. In our empirical study, nodes with low centrality have better forecasting ability. Furthermore, the least systemically important nodes can be predicted more accurately than the most systemically important nodes.

We explain these counterintuitive findings from the perspective of information theory. Our empirical results demonstrate that factors with low centrality have more useful information and less noise for the forecast asset price. While predicting a systemically important node, we show that other nodes within the network have a lower information rate.

In recent years, some scholars have combined complex networks and price predictions. Hu et al. (2022a) and Hu et al. (2022b) proposed efficient methods for predicting time series based on the visibility graph algorithm proposed by Lacasa et al. (2008) which transforms a time series into a complex network. Wang et al. (2016) presented another fast and simple computational method, the phase space coarse-graining algorithm, which converts a time series into a directed and weighted complex network, and applied it to analyze a gasoline spot price series. Subsequently, Wang et al. (2018), Wang et al. (2019) and Xu et al. (2020) forecast asset prices based on the above directed and weighted networks and obtained good prediction performance. Some scholars investigated the relationship between asset centrality and allocation. Pozzi et al. (2013) were the first to apply the topological structure and properties of financial networks to portfolio selection. In this approach, to avoid risks, more stocks located at the edge of the network should be configured. See Peralta and Zareei (2016), Vřrost et al. (2019) and Olmo (2021) for subsequent work. However, to the best of our knowledge, no study investigates the relationship between node centrality and the effectiveness of asset price prediction.

In this paper, we select 37 major global assets and construct complex networks based on the correlations between their prices. For problem (i), taking the London gold spot as a predicted target, we use first and last several central nodes as the influential factors to explore the effects of the factors' centrality on the prediction. We employ a hybrid random forest algorithm based on time-varying filtering-based

empirical mode decomposition (TVF-EMD-RF) to predict asset prices. By comparing the forecasting results of the three sets of first/last 6, 8, and 10 central nodes as factors, we find that all level accuracies using the last several central nodes are better than those using the first several central nodes. In particular, directional accuracies using the last several nodes as influential factors are generally 4%-6% higher than those using the first central nodes. Therefore, we conclude that factors with low centrality have better forecasting ability than those with high centrality. To provide a reasonable interpretation for the counterintuitive phenomenon, further empirical research employing information theory reveals that factors with low centrality have more useful information and less noise for the forecast asset price. For problem (ii), we select the assets with the most occurrences in the first and last 5 central nodes as the forecast nodes to analyze the impact of the forecast nodes' centrality on the prediction. When we forecast an asset price, we extract the first 10 principal components of the remaining 36 nodes as the influential factors. With the help of TVF-EMD-RF, we find that the least systemically important nodes can be forecast more accurately than the most systemically important nodes in terms of direction. The directional accuracies of the former are approximately 6%-8% higher than those of the latter. Using information theory again, we find that the former have higher *information rates*. This may provide a reasonable explanation for the finding. Finally, we use an alternative deep learning algorithm, TVF-EMD-DELM, to verify the robustness of our main conclusions.

The remainder of this paper is organized as follows. Section 2 introduces the main methods and concepts, including the complex network and eigenvector centrality, random forest, TVF-EMD algorithm, principal component analysis, and several concepts in information theory. Section 3 briefly introduces the data, network construction, forecasting approaches, and evaluation criteria. Section 4 explores the impact of the factors' centrality on the prediction. Section 5 explores the effects of the centrality of the forecast nodes on the prediction. Section 6 examines the robustness of our findings. Finally, Section 7 concludes the paper and discusses topics for future research.

2 Methodology

In this section, we briefly recall some concepts and algorithms, including complex networks and their centrality measures, random forest, TVF-EMD, principal component analysis, and several concepts of information theory.

2.1 Complex network and eigenvector centrality

Complex networks are graphs consisting of nodes and edges denoted as $G = (N, E)$. They can be divided into undirected and directed networks according to whether the edges have directions. They can be also divided into unweighted and weighted networks based on whether the edges are weighted.

To establish a complex network, an *adjacency matrix* $A = (a_{ij})_{n \times n}$ should be first constructed based

on a particular relationship among nodes, where n is the number of nodes and the element a_{ij} reflects the relationship between nodes i and j . A complex network constructed in this manner is fully connected. There are other construction methods, such as threshold networks, minimum spanning trees, and so on.

Topological properties or measures are important tools to analyze complex networks. Centrality measures can characterize the centrality and importance of the nodes in a network. For undirected weighted networks, *eigenvector centrality* is an applicable centrality measure (Peralta and Zareei (2016) and Olmo (2021)). The basic idea of eigenvector centrality is that the centrality of a node is a function of the centrality of its adjacent nodes (Bonacich (1972)). It is defined as follows,

$$EC_i = x_i = \frac{\sum_{j=1}^n a_{ij}x_j}{\lambda}, \quad (1)$$

where λ is the largest eigenvalue of A , and x is the eigenvector corresponding to λ of A , that is $Ax = \lambda x$. x_i , the i -th element of x , represents the eigenvector centrality of node i . This indicates that the importance of a node depends on the relationship between the node and its neighbors (nodes directly connected with it) and the importance of its neighbors.

2.2 Random forest

Ho (1995, 1998) developed the basic idea of random forest. As an ensemble learning model, random forest combines Breiman’s “bagging” idea (Breiman 1996) and a random selection of features. It takes the classification and regression trees (CARTs) as the basic model. CART is a binary decision tree (Breiman et al. 1984). For a classification problem, it uses the Gini index as a criterion to choose features and the splitting points. For a regression problem, it uses the mean square error (MSE) as a splitting criterion.

The final results of a random forest depend on the number of votes in all decision trees. For a classification problem, the random forest takes the majority vote of all decision trees as its result. For a regression problem, it uses the mean value. Random forest has the advantages of high speed and accuracy. More details are referred to Breiman (2001).

2.3 TVF-EMD

Researchers have developed many signal processing algorithms. Empirical mode decomposition (EMD) is a classic signal processing approach. Given an original signal $s(t)$, one can apply EMD to decompose it into different frequency bands in the time domain, known as intrinsic mode functions (IMFs). However, the method has the disadvantages of small end effects and mode aliasing. Li et al. (2017) proposed the TVF-EMD method based on time-varying filters, which is an adaptive algorithm that does not require a manual determination of the parameters. Compared with EMD, TVF-EMD can improve the frequency separation performance and stability at low sampling rates. In addition, the

proposed method is robust against noise interference. Therefore, we adopt TVF-EMD to decompose the price series in this paper.

2.4 Principal component analysis

Principal component analysis (PCA) is a popular technique for analyzing large datasets containing a high number of dimensions/features per observation. PCA is used to reduce the dimensionality of a dataset while preserving the maximum amount of information. It implies that the greater the variance, the greater the amount of information.

PCA using the covariance method requires the following steps (Pearson (1901) and Hotelling (1933)). (i) Centralize all original features. (ii) Calculate covariance matrix C . (iii) Find the eigenvalues of C and the corresponding eigenvectors. (iv) Select the largest first k eigenvalues and the corresponding eigenvectors. (v) Project the original features onto the selected eigenvectors and obtain new k -dimensional features after reducing the dimensions.

The percentage of the sum of the largest first k eigenvalues in the sum of all eigenvalues is called the contribution rate. Usually, the first several principal components with a certain contribution rate (such as 80%) or a certain number of the first several principal components are used.

2.5 Several concepts of information theory

(1) Shannon entropy and differential entropy

Shannon (1948) proposed the concept of *entropy*, where the entropy $H(X)$ of a discrete random variable X with possible values x_1, x_2, \dots, x_n and the probability mass function $P(X)$ is defined as

$$H(X) := - \sum_{i=1}^n P(x_i) \log_b P(x_i). \quad (2)$$

This reflects the expected amount of information of X . Otherwise, the entropy is also a measure of the uncertainty of a random variable. The common values of b are 2, 10, and e , and we use e as the base in this paper.

Correspondingly, *differential entropy* (also called continuous entropy) describes continuous probability distributions. Let X be a continuous random variable with a probability density function p whose support is a set \mathcal{X} . Its differential entropy $h(X)$ is defined as

$$h(X) := - \int_{\mathcal{X}} p(x) \ln p(x) dx. \quad (3)$$

It can be used to compare the uncertainty of two continuous random variables. Compared with the entropy of discrete random variables, the differential entropy can be negative and is not invariant under

continuous coordinate transformations. Therefore, we must compare the uncertainty of two continuous random variables at the same scale.

(2) Conditional entropy and conditional differential entropy

Conditional entropy quantifies the amount of information required to describe the outcome of a random variable Y given the value of another random variable X . The conditional entropy of two discrete random variables X and Y with possible values x_1, x_2, \dots, x_n and y_1, y_2, \dots, y_m , respectively, and the probability mass functions $P(X)$ and $P(Y)$, respectively, is defined as

$$H(Y|X) := - \sum_{i=1}^n \sum_{j=1}^m P(x_i, y_j) \ln \frac{P(x_i, y_j)}{P(x_i)},$$

where $P(X, Y)$ is the joint probability mass function of X and Y .

The continuous version of conditional entropy is called *conditional differential entropy*. Let X and Y be continuous random variables with values ranging in \mathcal{X} and \mathcal{Y} with a joint probability density function $p(x, y)$. Their marginal probability density functions are $p(x)$ and $p(y)$, respectively. The conditional differential entropy $h(Y|X)$ is defined as

$$h(Y|X) := - \int_{\mathcal{Y}} \int_{\mathcal{X}} p(x, y) \ln \frac{p(x, y)}{p(x)} dx dy. \quad (4)$$

(3) Mutual information

Mutual information is a measure of the mutual dependence between two random variables. The mutual information of the two discrete random variables X and Y is defined as

$$I(X; Y) := H(Y) - H(Y|X) = H(X) - H(X|Y) = \sum_{i=1}^n \sum_{j=1}^m P(x_i, y_j) \ln \frac{P(x_i, y_j)}{P(x_i)P(y_j)}.$$

It is equal to the difference between the entropy of Y and the conditional entropy $H(Y|X)$ and the difference between the entropy of X and the conditional entropy $H(X|Y)$.

The mutual information between two continuous random variables, X and Y , is defined as

$$I(X; Y) := h(Y) - h(Y|X) = h(X) - h(X|Y) = \int_{\mathcal{Y}} \int_{\mathcal{X}} p(x, y) \ln \frac{p(x, y)}{p(x)p(y)} dx dy. \quad (5)$$

It is equal to the difference between the differential entropy and conditional differential entropy.

The intuitive meaning of mutual information is the amount of information (i.e., reduction in uncertainty) that one variable provides to the other. Hence, mutual information is also known as information gain. Whether random variables are discrete or continuous, mutual information is non-negative, and

measures the true amount of information.

3 Data, approaches, and evaluation criteria

3.1 Data and complex network construction

We select 37 global assets, including 14 commodities, 14 stock indices, 6 currency rates, and 3 indicators (Dollar Index, RMB Index, VIX). Table 1 lists their names, categories, abbreviations, and data sources. In this paper, we use two sets of experimental data. The first testing set is from March 5, 2019 to April 28, 2020, and the second testing set is from February 5, 2021 to March 31, 2022. They are both 300 days.

Using sliding time windows, we construct dynamic complex networks of major global assets based on the absolute Pearson correlation coefficients between asset prices. At time t , we calculate correlation coefficients from $t - w + 1$ to t , where w is the window size. As is well known, for two series $u = \langle u_k \rangle$ and $v = \langle v_k \rangle$, their correlation coefficients are obtained in the following way (Feller (1971)),

$$\rho_t(u, v) := \frac{Cov_t(u, v)}{\sqrt{D_t(u)}\sqrt{D_t(v)}} = \frac{\sum_{k=t-w+1}^t (u_k - \bar{u})(v_k - \bar{v})}{\sqrt{\sum_{k=t-w+1}^t (u_k - \bar{u})^2} \sqrt{\sum_{k=t-w+1}^t (v_k - \bar{v})^2}},$$

where \bar{u} and \bar{v} are the mean values of the series u and v , respectively, in w days. At time t , the Pearson correlation coefficient matrix is defined as

$$Corr(t) = \begin{bmatrix} \rho_t(X_1, X_1) & \rho_t(X_1, X_2) & \cdots & \rho_t(X_1, X_l) & \rho_t(X_1, Y) \\ \rho_t(X_2, X_1) & \rho_t(X_2, X_2) & \cdots & \rho_t(X_2, X_l) & \rho_t(X_2, Y) \\ \cdots & \cdots & \cdots & \cdots & \cdots \\ \rho_t(X_l, X_1) & \rho_t(X_l, X_2) & \cdots & \rho_t(X_l, X_l) & \rho_t(X_l, Y) \\ \rho_t(Y, X_1) & \rho_t(Y, X_2) & \cdots & \rho_t(Y, X_l) & \rho_t(Y, Y) \end{bmatrix},$$

where X_1, X_2, \dots, X_l represent factors and Y represent the forecast series. We obtain the adjacency matrix with elements being the absolute value of each element of the matrix $Corr(t)$ because positive and negative correlations are equally important. Then, we calculate the eigenvector centrality of each node during each time window based on the adjacency matrix according to Eq. 1.

In this paper, we take a sliding window of 1,200 days, consistent with the length of the training sets when forecasting. Fig. 1 shows the asset network using data from August 18, 2017 to March 30, 2022. During this period, the first 10 central factors are the COMEX copper futures, SPTSX, S&P500, DAX30, N225, CRB comprehensive spot, KOSPI, CRB metal spot, CAC40, and London silver spot. The last 10 central factors are the HSI, VIX, USD effective exchange rate, dollar index, IBEX35, FISE100, FTMI, JP effective exchange rate, London brent crude, and EU effective exchange rate.

Table 1. Data categories and sources

Number	Category	Name	Abbreviation	Source
1	Commodity	London gold spot	LGS	https://www.wind.com.cn
2	Commodity	London silver spot	LSS	https://www.wind.com.cn
3	Commodity	London palladium spot	LPdS	https://www.kitco.com/gold.londonfix.html
4	Commodity	London platinum spot	LPtS	https://www.kitco.com/gold.londonfix.html
5	Commodity	COMEX gold futures	CGF	https://www.wind.com.cn
6	Commodity	COMEX silver futures	CSF	https://www.wind.com.cn
7	Commodity	COMEX copper futures	CCF	https://www.wind.com.cn
8	Commodity	ICE gold futures	IGF	https://www.wind.com.cn
9	Commodity	CRB metal spot	CMS	https://www.wind.com.cn
10	Commodity	CRB commodity index	CCI	https://www.wind.com.cn
11	Commodity	CRB comprehensive spot	CCS	https://www.wind.com.cn
12	Commodity	NYMEX gas futures	NGF	https://www.wind.com.cn
13	Commodity	NYMEX crude futures	NCF	https://www.wind.com.cn
14	Commodity	London Brent crude	LBC	https://www.wind.com.cn
15	Stock index	ASX200 (Australia)	ASX200	https://www.wind.com.cn
16	Stock index	SPTSX (Canada)	SPTSX	https://www.wind.com.cn
17	Stock index	CSI300 (China)	CSI300	https://www.wind.com.cn
18	Stock index	MOEX (Russia)	MOEX	https://www.wind.com.cn
19	Stock index	CAC40 (France)	CAC40	https://www.wind.com.cn
20	Stock index	HSI (Hong Kong)	HSI	https://www.wind.com.cn
21	Stock index	IBEX35 (Spain)	IBEX35	https://www.wind.com.cn
22	Stock index	FTMIB (Italy)	FTMIB	https://www.wind.com.cn
23	Stock index	KOSPI (Korea)	KOSPI	https://www.wind.com.cn
24	Stock index	FTMI (Singapore)	FTMI	https://www.wind.com.cn
25	Stock index	FISE100 (UK)	FISE100	https://www.wind.com.cn
26	Stock index	S&P500 (US)	S&P500	https://www.wind.com.cn
27	Stock index	N225 (Japan)	N225	https://www.wind.com.cn
28	Stock index	DAX30 (Germany)	DAX30	https://www.wind.com.cn
29	Economic indicator	VIX	VIX	https://www.wind.com.cn
30	Economic indicator	Dollar index	DI	https://www.wind.com.cn
31	Economic indicator	RMB index	RMBI	https://www.wind.com.cn
32	Economic indicator	UK effective exchange rate	UKR	https://www.bis.org/statistics/eer.htm
33	Economic indicator	USD effective exchange rate	USDR	https://www.bis.org/statistics/eer.htm
34	Economic indicator	EU effective exchange rate	EUR	https://www.bis.org/statistics/eer.htm
35	Economic indicator	CN effective exchange rate	CNR	https://www.bis.org/statistics/eer.htm
36	Economic indicator	JP effective exchange rate	JPR	https://www.bis.org/statistics/eer.htm
37	Economic indicator	Federal funds effective rate	FFR	https://www.federalreserve.gov

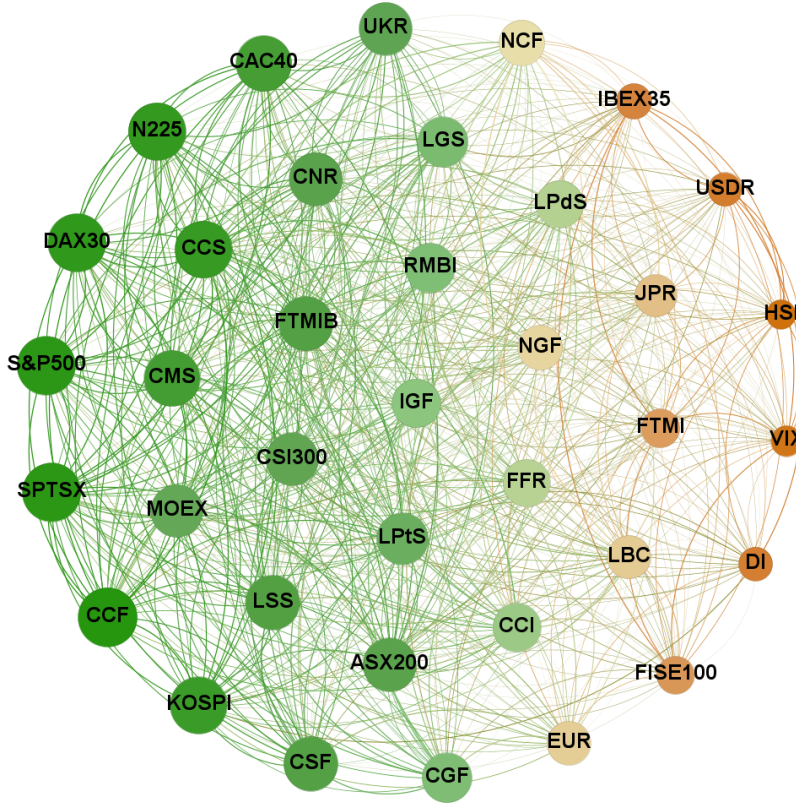


Fig. 1. Major global assets network. The nodes' labels are the asset abbreviations. The bigger a node and the darker green it is, the higher its eigenvector centrality and the more important it is in the complex network. The darker orange it is, the weaker is its centrality. The heavier the line, the greater its weight and the stronger the correlation between the two nodes. Otherwise, the color of a line is a mixture of the colors of the two nodes that it connects.

3.2 Forecasting approaches

To optimize the forecasting performance, we use machine learning algorithms with TVF-EMD in a rolling forecasting method. The rolling window is fixed for m days and recursively changes as the forecasting progresses in time (West (1996)). The steps are as follows: (i) Select proper influential factors as features according to the correlation or other criteria (the factors can vary) and historical a -day data of the forecast asset price. (ii) Divide the dataset into the training and testing sets. For the rolling forecasting model, the previous m -day data of the forecast day are set as the training set. (iii) For each window, we extract a fixed amount of IMFs from the forecast time series using TVF-EMD. (iv) Forecast each IMF using machine learning algorithms and sum the forecast values as the final forecast value.

Considering the training cost and model evaluation requirements, the rolling forecasting time of each set in this paper is 300 days, with the training set lasting 1,200 days ($m = w = 1200$). To forecast the

asset price at time t , we use its historical 2-day prices ($a = 2$).

3.3 Evaluation criteria

In this paper, we focus mainly on the directional accuracy. The direction statistic is defined in Eq.

6. The larger the value, the more accurate the forecasting results.

$$D_{stat} = \frac{\sum_{t=1}^T I_t}{T} \times 100\%, \quad (6)$$

where

$$I_t = \begin{cases} 1, & \text{if } (Y_t - Y_{t-1})(\hat{Y}_t - Y_{t-1}) \geq 0; \\ 0, & \text{if } (Y_t - Y_{t-1})(\hat{Y}_t - Y_{t-1}) < 0. \end{cases}$$

T is the number of elements in the testing set, Y_t is the true value of the testing sample, and \hat{Y}_t is the forecast value at time t .

To fully compare the forecasting results, we also use MAPE, MAE, RMSE and R^2 to evaluate the prediction accuracy (see Table 2). A high R^2 value is preferable for the prediction. For the other three criteria, lower values indicate more accurate forecasting results.

Table 2. Accuracy evaluation criteria

Evaluation criteria	Abbreviation	Formula
Mean absolute percentage error	MAPE	$\frac{1}{T} \sum_{t=1}^T \left \frac{\hat{Y}_t - Y_t}{Y_t} \right $
Mean absolute error	MAE	$\frac{1}{T} \sum_{t=1}^T \hat{Y}_t - Y_t $
Root mean square error	RMSE	$\sqrt{\frac{1}{T} \sum_{t=1}^T (\hat{Y}_t - Y_t)^2}$
Goodness of fit	R^2	$1 - \frac{\sum_{t=1}^T (\hat{Y}_t - Y_t)^2}{\sum_{t=1}^T (Y_t - \bar{Y})^2}$

4 The impact of factors' centrality on prediction

In this section, we take London gold spot as the forecast node to analyze the impact of the factors' centrality on the forecasting results.

4.1 Forecasting results using different central factors

We can use complex networks to extract features. To forecast the price at time t , we select features according to the eigenvector centrality of each node at time $t - 1$ because the data at time t cannot be known in advance. We construct the network at time $t - 1$ using the 1,200-day data from $t - 1200$

to $t - 1$. Evidently, the eigenvector centrality of each node in the asset network changes daily, and it reflects the importance (status) of these nodes during the previous window.

In order to discuss the impact of the factors' centrality on the forecasting results, we consider a special case where we use the first 6, 8, and 10 central nodes and the last 6, 8, and 10 central nodes, except the London gold spot, as its influential factors every day and compare their forecasting results for the full testing set (300 days). Table 3 reports the results for the two experimental datasets obtained by TVF-EMD-RF.

Table 3. Forecasting results of the London gold spot price obtained by TVF-EMD-RF

Testing set	Factors	Dstat (%)	MAPE (%)	MAE	RMSE
2019/3/5-2020/4/28	First 6 central factors	54.33	1.06	15.97	23.77
	Last 6 central factors	59.67	0.95	14.39	21.77
	First 8 central factors	55.67	1.01	15.21	21.83
	Last 8 central factors	61.67	0.95	14.30	20.68
	First 10 central factors	55.00	1.12	16.97	25.99
	Last 10 central factors	59.00	1.07	16.21	22.44
2021/2/5-2022/3/31	First 6 central factors	54.67	0.89	16.18	22.31
	Last 6 central factors	59.00	0.83	14.96	20.47
	First 8 central factors	57.33	0.89	16.10	21.86
	Last 8 central factors	62.00	0.87	15.79	21.70
	First 10 central factors	55.67	0.88	15.91	21.75
	Last 10 central factors	59.67	0.85	15.52	21.23

In Table 3, the last 6, 8, and 10 central factors have better forecasting performance in terms of both directional and level accuracy than the first 6, 8, and 10 central factors do, respectively. Directional accuracies using the last several factors are generally 4%-6% higher than those using the first several factors. MAPEs using the last several factors are 0.02%-0.11% lower than those using the first several factors. Taking the first dataset for instance, the directional accuracy when using the last 8 central factors is 61.67%, which is 6.00% higher than that when using the first 8 central factors. Hence, factors' centrality has a significant effect on the prediction.

Therefore, we conclude that factors with low centrality have better forecasting effects on the same asset than those with high centrality do. High centrality of nodes in a complex network is not equivalent to strong correlation between nodes and the forecast target. The results are not contradictory to the traditional selection of factors based on correlation. Moreover, they suggest a new idea for selecting factors. When predicting an asset price in a complex system, factors with low centrality should be selected rather than only factors with high centrality.

In the remainder of this section, we aim to explain our main conclusions from an information perspective.

4.2 PCA for the selected factors

We perform a PCA for factors with high centrality and those with low centrality for the two datasets.

For each testing sample, we extract the principal components of the first/last 6, 8, and 10 central factors from its training set and itself (1201 days) and record their quantities at various contribution rates. Then, we obtain the time series data (including 300 days) for every experimental dataset regarding the number of principal components for the first/last central factors. Fig. 2 shows the average quantities of the principal components in the first dataset.

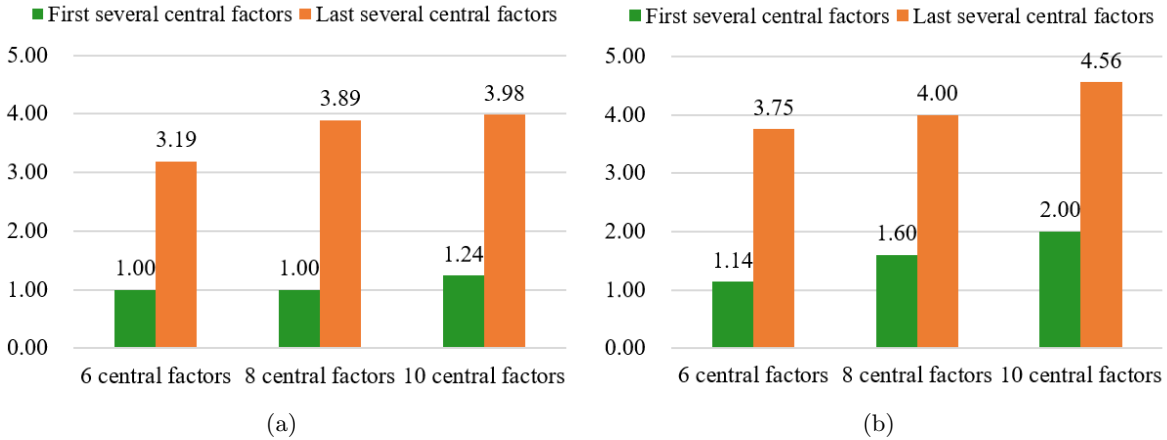


Fig. 2. Average quantities of principal components in the first dataset. (a). At 80% contribution rates; (b). At 85% contribution rates.

In Fig. 2, the factors with low centrality always have more principal components than those with high centrality for the same quantity of factors at the same contribution rate. For example, in the first dataset, the first 8 central factors have only one principal component at the 80% contribution rate, whereas the last 8 central factors have 3.89 principal components. Results for the second dataset are similarly. Hence, it is possible that the factors with high centrality include less information. This may be because factors with high centrality have high correlations among themselves, so they have fewer principal components, and thus include a small amount of information.

4.3 Estimating entropy and mutual information of factors and the forecast node

To the best of our knowledge, the PCA method considers only the information that factors include, focusing on the relationship among factors and ignoring the relationship between factors and the forecast asset. Selecting features with maximal relevance and minimal redundancy is a good feature selection

approach, and features selected in this manner usually have good prediction or classification results (Peng et al. (2005); Ding et al. (2005)). Relevance is typically characterized in terms of correlation or mutual information. Therefore, to further explore why factors with low centrality can better predict gold prices, we analyze them from the perspective of information theory.

Let \mathbf{X} denote the factors and Y denote the gold price. We use the Gaussian kernel density method to estimate the differential entropy (Ahmad et al. 1976) of \mathbf{X} and Y and mutual information (Moon et al. 1995) between \mathbf{X} and Y to measure the effectiveness of factors in the prediction of the gold price.

First, we estimate the differential entropy of the gold price under a rolling window (1,201 days) based on Eq. 3. We obtain a time series of 300 days for each experimental dataset. The average differential entropy is 5.86 from 2019/3/5 to 2020/4/28, and it is 6.76 from 2021/2/5 to 2022/3/31. The average differential entropy of the second dataset is larger than that of the first dataset, indicating that the uncertainty of the price is greater in the second dataset.

Second, to obtain the amount of information that a set of factors X_1, X_2, \dots, X_n provides to the forecast asset Y , we need to estimate the mutual information $I(X_1, X_2, \dots, X_n; Y)$ between these factors and the forecast asset, instead of the sum of the mutual information between a single factor X_i and Y , that is $\sum_{i=1}^n I(X_i, Y)$. Because the mutual information between X_i and Y and that between X_j and Y ($i \neq j$) may overlap according to Eq. 5. The equation of mutual information (continuous version) between n factors X_1, X_2, \dots, X_n and Y with value ranges $\mathcal{X}_1, \mathcal{X}_2, \dots, \mathcal{X}_n$ and \mathcal{Y} is written as

$$\begin{aligned} I(\mathbf{X}; Y) &= I(X_1, X_2, \dots, X_n; Y) \\ &= h(X_1, X_2, \dots, X_n) - h(X_1, X_2, \dots, X_n|Y) \\ &= \int_{\mathcal{X}_1} \int_{\mathcal{X}_2} \dots \int_{\mathcal{X}_n} \int_{\mathcal{Y}} p(x_1, x_2, \dots, x_n, y) \ln \frac{p(x_1, x_2, \dots, x_n, y)}{p(x_1, x_2, \dots, x_n)p(y)} dx_1 dx_2 \dots dx_n dy, \end{aligned} \quad (7)$$

where $p(x_1, x_2, \dots, x_n)$ and $p(x_1, x_2, \dots, x_n, y)$ are the joint probability density functions of \mathbf{X} and (\mathbf{X}, Y) , respectively. The greater the mutual information $I(\mathbf{X}; Y)$ between some factors and the gold price, the larger the amount of information the factors have about the London gold spot price.

Furthermore, we should consider the proportion of valid to invalid information that n factors bring to the forecast target. The larger the amount of invalid information, the greater the interference to forecast Y . We regard the remainder of the differential entropy of n factors minus the mutual information $I(\mathbf{X}; Y)$ as noise. That is, the noise is $h(\mathbf{X}|Y)$. We then define the *information/noise ratio* of \mathbf{X} to Y as

$$I/N = \frac{I(\mathbf{X}; Y)}{h(\mathbf{X}|Y)} \times 100\% = \frac{I(X_1, X_2, \dots, X_n; Y)}{h(X_1, X_2, \dots, X_n|Y)} \times 100\%. \quad (8)$$

Evidently, I/N is positively related to $I(\mathbf{X}; Y)$ and negatively related to the conditional differential entropy of n factors.

From the information perspective, the ideal situation is that the information that the factors provide

to the forecast asset price Y exactly equals the information of Y (the entropy of Y). That is, the factors of Y have no interference. Thus, the directional accuracy will be 100%, and the error will be 0.

We use mutual information and the information/noise ratio to evaluate the effectiveness of the factors \mathbf{X} in forecasting Y . Because the factors change daily, the mutual information and the information/noise ratio also change. We calculate the average differential entropy of factors, mutual information between the first/last 8 central factors and the forecast asset, conditional differential entropy, and information/noise ratio for each testing set, as we report in Table 4.

Table 4. Average differential entropy, mutual information, conditional differential entropy, and information/noise ratio

Testing set	Factors	$h(\mathbf{X})$	$I(\mathbf{X}; Y)$	$h(\mathbf{X} Y)$	I/N
2019/3/5-2020/4/28	First 8 central factors	48.96	1.42	47.54	2.99%
	Last 8 central factors	14.48	1.49	12.98	11.67%
2021/2/5-2022/3/31	First 8 central factors	43.74	1.47	42.27	3.48%
	Last 8 central factors	27.22	1.52	25.72	6.70%

The last 8 central factors have both more average mutual information and a higher average information/noise ratio for the London gold spot price than the first 8 central factors do in the two datasets. It indicates that factors with low centrality have more effective information and less noise than those with high centrality do. This may partially explain why the last central factors can better predict the same asset price.

Taking the first dataset as an example, Fig. 3 depicts the daily $I(\mathbf{X}; Y)$ and I/N . During these 300 days, the mutual information between the last 8 central factors and the London gold spot price is larger than that between the first 8 central factors and the gold spot price for 169 days. However, the average of the former is larger than that of the latter. The information/noise ratio of the last 8 central factors is always significantly higher than that of the first 8 central factors. Therefore, we believe that the information/noise ratio of the factors may be more important than mutual information in a forecasting problem. Additionally, we see some dramatic changes in the figure owing to the substitution of some factors. The phase of slight changes in $I(\mathbf{X}; Y)$ and I/N is caused mainly by the fluctuation of prices.

5 Impact of forecast node’s centrality on prediction

Compared with Section 4, where we examined the impact of the factors’ centrality on prediction, we study the impact of the forecast asset’s centrality on forecasting results in this section.

For the two datasets, we take the assets with the most occurrences in the first/last 5 central nodes as the forecast nodes for 300 days. Every complex network is constructed using 1200-day data before a

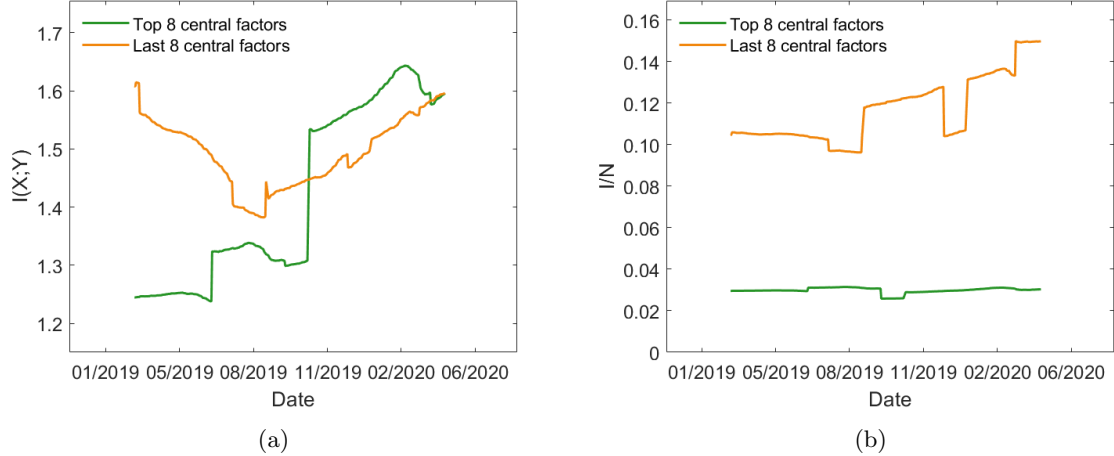


Fig. 3. Mutual information and information/noise ratio in the first dataset. (a). $I(\mathbf{X};Y)$; (b). I/N .

testing sample. According to these criteria, we obtain the most systemically important nodes, the least systemically important nodes, and their times of occurrence during 300 days, as shown in Table 5.

Table 5. The most and least systemically important nodes in the two datasets

Testing set	2019/3/5-2020/4/28	2021/2/5-2022/3/31
Most systemically important nodes	SPTSX (300) FISE100 (300)	S&P500 (243)
Least systemically important nodes	London silver spot (300) COMEX silver futures (300)	VIX (241)

Numbers in parentheses behind assets represent the times which the assets belong to the first or last 5 central nodes in the datasets.

In the first dataset, the SPTSX (Canada) and FISE100 (UK) always belong to the first 5 central nodes, and the London silver spot and COMEX silver futures always belong to the last 5 central nodes. In the second dataset, the S&P500 (US) and VIX have the most occurrences, though they belong to the first or last 5 central nodes for only 80% of the 300 trading days. Fig. 4 shows the complex network on April 4, 2019.

5.1 Forecasting results for different central nodes

We forecast each asset using TVF-EMD-RF. When forecasting an asset, we take the other 36 assets as factors. Considering their overabundance, we extract the first 10 principal components as the actual factors. The cumulative variance contribution rates of them when predicting these assets are all between 97% and 98%. Equivalently, we use almost equal information to predict these nodes. Because MAE

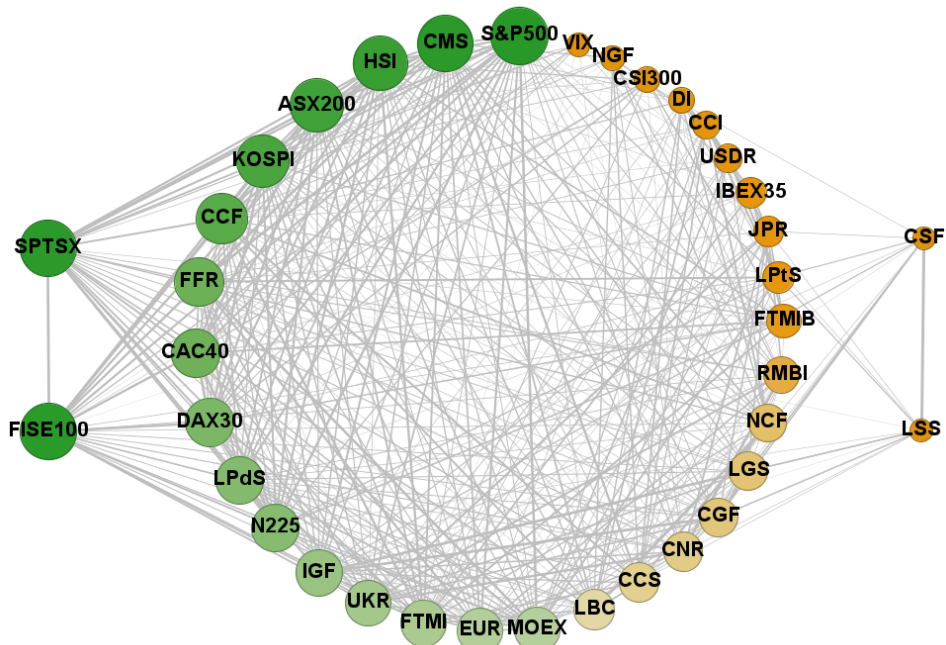


Fig. 4. Network on April 4, 2019. The SPTST and FISE100 have the highest eigenvector centrality and are on the far left. The London silver spot and COMEX silver futures with the lowest eigenvector centrality are on the far right. To show the relationship between nodes more clearly, we have hidden the edges with weights below 0.3.

and RMSE are not comparable when forecasting various assets, we use MAPE and R^2 as the evaluation criteria for level accuracy. Furthermore, we employ the coefficient of variation (CV) to measure the degree of dispersion of their prices, which is defined as the ratio of the standard deviation to the mean. Table 6 lists the forecasting results of the two most and two least systemically important nodes in the first dataset.

Table 6. Forecasting results of different central assets in the first dataset obtained by TVF-EMD-RF

Centrality	Forecast asset	Dstat (%)	MAPE (%)	R^2	CV
Most systemically important nodes	SPTSX	55.33	1.01	0.9387	0.0716
	FISE100	55.00	1.07	0.9661	0.0845
Least systemically important nodes	London silver spot	63.00	1.57	0.9248	0.0875
	COMEX silver futures	61.67	1.67	0.8998	0.0875

Evidently, the directional accuracies of the least systemically important nodes are approximately 6%-8% higher than those of the most systemically important nodes. However, their level accuracies are the opposite. From Table 6, we find that the two least systemically important nodes are associated with a greater MAPE and lower R^2 relative to the two most systemically important nodes. The poor

performance in terms of the level accuracy of the two least systemically important nodes may be caused by their large CVs. As we know, it is difficult to obtain a good level accuracy when predicting asset prices with high volatility (Lu et al. (2023)).

To explain the opposite directional and level accuracy results, we first conduct an experiment to forecast two geometric Brownian motions with zero drift, but different volatilities. We use only the historical path to predict future values. We obtain both about 50% of the directional accuracies, but notably different level accuracies. The geometric Brownian motion with lower volatility has a higher level accuracy. Then we forecast several sets of geometric Brownian motions with different drifts and volatilities. For geometric Brownian motions with different drift terms but the same volatilities, the geometric Brownian motion with high drift has a higher direction statistic, but their level accuracies are almost the same. The drift term can be understood as information to some extent. Hence, we conclude that the direction statistic is mainly affected by the factors' information, whereas level accuracy is determined by both the forecast asset's volatility and the factors' information.

These observations are also supported by our empirical analysis of the second dataset, which we report in Table 7.

Table 7. Forecasting results of different central assets in the second dataset obtained by TVF-EMD-RF

Centrality	Forecast asset	Dstat (%)	MAPE (%)	R ²	CV
Most systemically important node	S&P500	54.33	1.07	0.9376	0.0565
Least systemically important node	VIX	61.33	7.49	0.7300	0.2154

5.2 Cause analysis from information perspective

We attempt to explain and analyze the above conclusions from the perspective of information in this subsection.

We estimate the mutual information between factors (10 principal components) and the forecast assets; however, because the forecast assets are different, we must consider their differential entropy. Therefore, we define the *information rate* as the ratio of mutual information to differential entropy, that is

$$IR = \frac{I(\mathbf{X}; Y)}{h(Y)} \times 100\% = \frac{I(X_1, X_2, \dots, X_n; Y)}{h(Y)} \times 100\%. \quad (9)$$

It reflects the interpretable level of factors X_1, X_2, \dots, X_n to the forecast asset Y . To some extent, IR implies the proportion of the amount of useful information to the forecast asset price that we can extract from the factors.

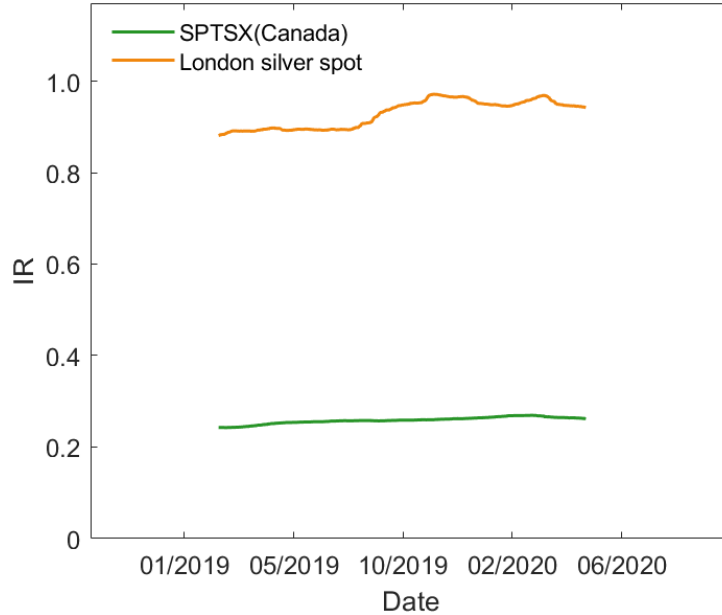
Table 8 shows the average results of the mutual information, differential entropy of the forecast assets, and information rate in the 300-day testing samples for the two datasets, respectively.

Table 8. Average mutual information, differential entropy and information rate

Testing set	Asset (Y)	$I(\mathbf{X}; Y)$	$h(Y)$	IR
2019/3/5-2020/4/28	SPTSX	2.00	8.25	24.25%
	FISE100	2.11	7.63	27.70%
	London silver spot	1.57	1.78	88.08%
	COMEX silver futures	1.56	1.79	87.53%
2021/2/5-2022/3/31	S&P500	2.62	7.43	35.28%
	VIX	1.37	3.38	40.65%

According to Table 8, the most systemically important assets have more mutual information with factors; moreover, their entropy is much greater than that of the least systemically important assets. It shows that the most systemically important nodes themselves have more information. However, the proportion of the mutual information to the entropy of the forecast node $I(\mathbf{X}; Y)/h(Y)$ is lower. In other words, the IR of the most systemically important nodes is lower than that of the least systemically important nodes. This phenomenon is more pronounced in the first dataset than in the second dataset.

Fig. 5 illustrates the dynamic information rates of the SPTSX and London silver spot in the first testing set. The information rate of the London silver spot is always higher than that of the SPTSX.

**Fig. 5.** Dynamic information rates of the SPTSX (the most systemically important node) and London silver spot (the least systemically important node).

Therefore, we conclude that the directional accuracies of the least systemically important nodes tend

to be better than those of the most systemically important nodes in a close complex system because the first 10 principal components of the other 36 assets, except the forecast node, have a higher information rate to the least systemically important nodes.

6 Robustness analysis

In Sections 4 and 5, we have used two datasets to demonstrate the robustness of the conclusions on time scales. To eliminate the contingency of the method, we use a deep extreme learning machine based on time-varying filtering-based empirical mode decomposition (TVF-EMD-DELM) to forecast asset prices. The forecasting procedures are consistent with those presented in Sections 4 and 5.

Table 9 shows the forecasting results for the London gold spot price using different central factors in the two datasets. Factors with low centrality apparently have better prediction effects on the London gold spot price, which supports the conclusion in Section 4.

Table 9. Forecasting results of the London gold spot price obtained by TVF-EMD-DELM

Testing set	Factors	Dstat (%)	MAPE (%)	MAE	RMSE
2019/3/5-2020/4/28	First 6 central factors	54.67	0.94	14.16	21.92
	Last 6 central factors	59.00	0.85	12.80	18.85
	First 8 central factors	54.33	0.94	14.18	22.01
	Last 8 central factors	59.00	0.89	13.28	19.04
	First 10 central factors	55.33	0.94	14.22	22.64
	Last 10 central factors	60.67	0.93	13.98	20.34
2021/2/5-2022/3/31	First 6 central factors	55.00	0.83	15.02	20.50
	Last 6 central factors	57.67	0.81	14.81	20.52
	First 8 central factors	54.00	1.00	18.09	24.07
	Last 8 central factors	59.33	0.94	17.17	24.16
	First 10 central factors	54.00	1.00	18.16	26.67
	Last 10 central factors	59.00	0.98	17.68	24.32

To verify the robustness of the results in Section 5, Table 10 displays the forecasting results of the different central assets in the two datasets using TVF-EMD-DELM. The directional accuracies of the least systemically important nodes is 4%-8% higher than that of the most systemically important nodes, consistent with our conclusions in Section 5.

Therefore, our findings are robust.

Table 10. Forecasting results of different central assets obtained by TVF-EMD-DELM

Testing set	Centrality	Forecast asset	Dstat (%)	MAPE (%)	R^2
2019/3/5-2020/4/28	Most systemically important nodes	SPTSX	54.67	1.03	0.9378
		FISE100	53.67	1.13	0.9619
	Least systemically important nodes	London silver spot	59.33	1.50	0.9271
		COMEX silver futures	61.00	1.51	0.9244
2021/2/5-2022/3/31	Most systemically important nodes	S&P500	52.67	1.08	0.9408
	Least systemically important nodes	VIX	60.67	7.61	0.7280

7 Conclusion

This paper studies the impacts of node centrality on the asset price prediction in networks of major global assets from two aspects: factors' centrality and the forecast node's centrality. We obtain two interesting conclusions. First, factors with low centrality tend to have better forecasting outcomes than those with high centrality do when forecasting the same asset. Second, the least systemically important nodes tend to be predicted more accurately than the most systemically important nodes in terms of directional accuracies. We verified the robustness of these conclusions using different datasets and different machine learning methods.

We explain these phenomena from the perspective of information. On the one hand, with the help of PCA and information theory, we find that factors with low centrality have more effective information for the forecast asset. We define the information/noise ratio and find that factors with low centrality have a high information/noise ratio. Furthermore, the information/noise ratio is more important than the mutual information when forecasting the same asset. On the other hand, we define the information rate and find that although other assets have more mutual information with the most systemically important nodes than with the least systemically important nodes, the information rate plays a crucial role in directional accuracy for the different forecast assets.

Nodes with high centrality are typically important. For instance, the risk of a bank system is almost decided by its systemically important banks. However, our conclusions indicate that the lower the centrality of the factors and the forecast node, the better the performance of the forecasting results.

One direction for future work is to expand the application of our findings to networks consisting of non-financial assets to obtain more general conclusions. Another possibility is to consider the various relationships among the nodes and alternative measures.

References

- Han M, Fan Q, Ling G. Multiscale online-horizontal-visibility-graph correlation analysis of financial market. *Physica A: Statistical Mechanics and its Applications*, 2022: 128195.
- Wang G J, Xie C, Stanley H E. Correlation structure and evolution of world stock markets: Evidence from Pearson and partial correlation-based networks. *Computational Economics*, 2018, 51(3): 607-635.
- Battiston S, Caldarelli G, May R M, et al. The price of complexity in financial networks. *Proceedings of the National Academy of Sciences*, 2016, 113(36): 10031-10036.
- Yu J, Zhao J. Prediction of systemic risk contagion based on a dynamic complex network model using machine learning algorithm. *Complexity*, 2020: 1-13.
- Ma X, Deng W, Qiao W, et al. A novel methodology concentrating on risk propagation to conduct a risk analysis based on a directed complex network. *Risk Analysis*, 2022. <https://doi.org/10.1111/risa.13870>.
- Pozzi F, Di M T, Aste T. Spread of risk across financial markets: better to invest in the peripheries. *Scientific Reports*, 2013, 3(3): 1665.
- Peralta G, Zareei A. A network approach to portfolio selection. *Journal of Empirical Finance*, 2016, 38: 157-180.
- Výrost T, Lyócsa Š, Baumöhl E. Network-based asset allocation strategies. *The North American Journal of Economics and Finance*, 2019, 47: 516-536.
- Olmo J. Optimal portfolio allocation and asset centrality revisited. *Quantitative Finance*, 2021, 21(9): 1475-1490.
- Adamic L, Brunetti C, Harris J H, et al. Trading networks. *The Econometrics Journal*, 2017, 20(3): S126-S149.
- Musciotto F, Piilo J, Mantegna R N. High-frequency trading and networked markets. *Proceedings of the National Academy of Sciences*, 2021, 118(26): e2015573118.
- Chen W, Hou X, Jiang M, et al. Identifying systemically important financial institutions in complex network: A case study of Chinese stock market. *Emerging Markets Review*, 2022, 50: 100836.
- Kuzubas T U, Ömercikoğlu I, Saltoğlu B. Network centrality measures and systemic risk: An application to the Turkish financial crisis. *Physica A: Statistical Mechanics and its Applications*, 2014, 405: 203-215.
- Lacasa L, Luque B, Ballesteros F, et al. From time series to complex networks: The visibility graph. *Proceedings of the National Academy of Sciences*, 2008, 105(13): 4972-4975.
- Hu Y, Xiao F. An efficient forecasting method for time series based on visibility graph and multi-subgraph similarity. *Chaos, Solitons & Fractals*, 2022, 160: 112243.
- Hu Y, Xiao F. A novel method for forecasting time series based on directed visibility graph and improved random walk. *Physica A: Statistical Mechanics and its Applications*, 2022, 594: 127029.
- Wang M, Tian L. From time series to complex networks: The phase space coarse graining. *Physica A: Statistical Mechanics and its Applications*, 2016, 461: 456-468.
- Wang M, Zhao L, Du R, et al. A novel hybrid method of forecasting crude oil prices using complex network science and artificial intelligence algorithms. *Applied Energy*, 2018, 220: 480-495.
- Wang C, Zhang X, Wang M, et al. Predictive analytics of the copper spot price by utilizing complex network and artificial neural network techniques. *Resources Policy*, 2019, 63: 101414.

- Xu H, Wang M, Jiang S, et al. Carbon price forecasting with complex network and extreme learning machine. *Physica A: Statistical Mechanics and its Applications*, 2020, 545: 122830.
- Bonacich P. Factoring and weighting approaches to status scores and clique identification. *Journal of Mathematical Sociology*, 1972, 2(1): 113-120.
- Ho T K. Random decision forests. *Proceedings of 3rd international conference on document analysis and recognition*. IEEE, 1995, 1: 278-282.
- Ho T K. The random subspace method for constructing decision forests. *IEEE Transactions on Pattern Analysis and Machine Intelligence*, 1998, 20(8): 832-844.
- Breiman L. Bagging predictors. *Machine Learning*, 1996, 24(2): 123-140.
- Breiman L, Friedman J H, Olshen R A, et al. Classification and regression trees (CART). *Biometrics*, 1984, 40(3): 358-361.
- Breiman L. Random forests. *Machine Learning*, 2001, 45(1): 5-32.
- Li H, Li Z, Mo W. A time varying filter approach for empirical mode decomposition. *Signal Processing*, 2017, 138: 146-158.
- Pearson K. LIII. On lines and planes of closest fit to systems of points in space. *The London, Edinburgh, and Dublin Philosophical Magazine and Journal of Science*, 1901, 2(11): 559-572.
- Hotelling H. Analysis of a complex of statistical variables into principal components. *Journal of Educational Psychology*, 1933, 24(6): 417.
- Shannon C E. A mathematical theory of communication. *The Bell System Technical Journal*, 1948, 27(3): 379-423.
- Feller W. *An introduction to probability theory and its applications*. Wiley, New York, 1971.
- West K D. Asymptotic inference about predictive ability. *Econometrica*, 1996, 64(5): 1067-1084.
- Peng H, Long F, Ding C. Feature selection based on mutual information criteria of max-dependency, max-relevance, and min-redundancy. *IEEE Transactions on Pattern Analysis and Machine Intelligence*, 2005, 27(8): 1226-1238.
- Ding C, Peng H. Minimum redundancy feature selection from microarray gene expression data. *Journal of Bioinformatics and Computational Biology*, 2005, 3(02): 185-205.
- Ahmad I, Lin P E. A nonparametric estimation of the entropy for absolutely continuous distributions (corresp.). *IEEE Transactions on Information Theory*, 1976, 22(3): 372-375.
- Moon Y I, Rajagopalan B, Lall U. Estimation of mutual information using kernel density estimators. *Physical Review E*, 1995, 52(3): 2318.
- Lu Z, Xu Y, Zhang Y. Predicting asset price with large volatility: a case study of Bitcoin. Working paper, 2023.